R. El-Saifi et al., J. Al-Aqsa Unv., 10 (S.E) 2006

Band reject filter of a periodic dielectric film bounded by a nonlinear cladding

Mr. Rafek N. El-Saifi*
Dr. Hala. J. El-Khozondar **
Prof. Mohammed M. Shabat ***

الملخص

مرشح نبذ نطاقي لشريحة رقيقة عازلة دورية معامل النفاذية ومحدودة بتغليف غير خطي النفاذية

تم دراسة انتشار الموجات الكهربية المستعرضة (TE) خلال ثـلاث طبقـات بنفاذيـة مختلفة عبارة عن وسط غير خطي دوري محاط من أعلاه بمادة غير خطية ومـن أسـفل بمـادة خطية، ومن خلال الدراسة استخدمنا معادلات ماكسويل، والشروط الحدية لاشتقاق معادلة التـشتت (Dispersion Equation)، استخدمنا في هذه الدراسـة دوال مـاثيو (Mathieu Functions) كحـل مـضبوط وطـرق الاضـطراب (Perturbation Methods) بطـريقتين الأولـى (Whittaker's Method) و الثانية (Multiple Scales Method)، وقد لاحظنا التوافق الكبير بين هذه الطرق،وقد استخدمنا البرنامج الرياضي (Maple 9) لحساب ورسم طاقة الموجة كدالـة في معامل الانكسار الفعال β فمن الرسم لاحظنا أن طاقة الموجة تزداد بزيادة معامـل الانكـسار الفعال، وعند رسم طاقة الموجة كدالة في التردد لاحظنا أن طاقة الموجة تظهر (pass band) ثـم تختفي (stop band) ثم تظهر (pass band) لتردد مختلف، ولهذا يمكن اسـتخدام النظـام كمصفي (a band reject filter)، ومن خلال هـذا البحـث لاحظنـا أن الطـرق الاضـطراب (Perturbation Methods) من أفضل الطرق لحل هذه المسائل من حيث الجهد وتوفير الوقـت، ولاختيار المواد المناسبة ذات الجودة والكفاءة العالية،التي تستخدم في كثير من الأجهزة الفيزيائيـة في الصناعة.

---

* Mathematics Department, Al-Aqsa University, Gaza, Palestine, r.saify@upi.ps
**Department of Electrical and Computer Engineering, Islamic University, Gaza, P.O. Box 108, Gaza Strip, Palestine, hkhozondar@mail.iugaza.edu.ps
***Department of Physics, Islamic University, Gaza, P. O. Box 108, , Gaza Strip, Palestine, shabat@mail.iugaza.edu.ps

ABSTRACT

Two perturbation analytical methods have been developed to study the behavior of electromagnetic in a periodic dielectric film bounded by a nonlinear cladding and a dielectric substrate. A simple numerical method has also been applied based on Mathieu function approach. Numerical results have been presented, we found that the approximate techniques are much easier and faster, and the considered wave guide structure represents a band reject filter.

Keywords: nonlinear optics, stratified media, Mathieu function, multiple scale method, Whittaker's method, filter.

INTRODUCTION:

This study focuses on understanding the behavior of electromagnetic field in a medium possessing a dielectric constant which is sinusoidally stratified along one coordinate sandwiched between a nonlinear cladding and a linear dielectric substrate. A first area of application is concerned with TE wave propagation through a compressible medium which is influenced by acoustic or other mechanical wave. As an example, the results are applicable to acoustically modulated plasma media in range of frequencies above plasma frequency. A second area of application regards the stratified medium as a first step in analysis of a sinusoidally modulated dielectric slab antenna. The power has been calculated by using Mathieu equation and using perturbation methods (Whittaker's Method, and Multiple Scale Method).

The propagation of waves in periodically stratified media was discussed as early as 1887 by Lord Rayleigh [1], who recognized that this electromagnetic problem was characterized by the Hill and Mathieu differential equations. It should also be mentioned that, both before and after Lord Rayleigh, the Hill and Mathieu equations have been investigated in other applications, including the vibration of strings and sheets with specified mass distributions. The propagation of TE waves in semi-infinite nonlinear medium is chosen to have a dielectric constant that depends on the field intensity. Such media have been studied by many authors [2-7]. The periodic media has been investigated by a number of authors [11–14]. In our previous work [13], we have investigated the behavior of nonlinear surface waves guided by a single periodic medium. In this communications, we extended the previous work to study the behavior of nonlinear cladding.

The Geometry of the problem:

The geometry of the problem is shown in Figures (1) medium-1 extends to infinity in xy-plane and restricted to z ≥0 and the relative permittivity of the cladding (nonlinear medium) is taken to be dependent on the field intensity of the waves as [7]:

$$\varepsilon_{m1} = \varepsilon_1 + \alpha\ |E\ |^2$$

Where ε_1 is linear and α is the strength of the nonlinear effect. Medium 2, the stratified layer (film), has a periodic structure of the relative dielectric function (permittivity) of [11-13],

$$\varepsilon_{m2} = \varepsilon_2 + \Delta \cos \delta z$$

where ε_2 is average ε_{m2} and Δ is the modulation index, and $\Delta \leq \varepsilon_2$ and where δ is related to the period of the stratified modulation Λ by $\delta = 2\pi / \Lambda$. The medium restricted to $-d \leq z \leq 0$ is visualized as consisting of layers parallel to the xy-plane and spaced by a distance Λ.

Medium-3, linear layer (substrate), extends to infinity in xy-plane and restricted to z ≤ -d has relative dielectric function (permittivity) ε_3**.**

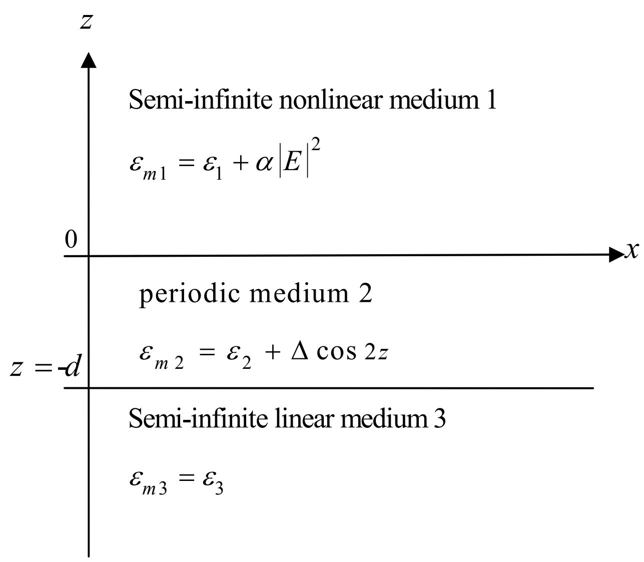

Figure1. The geometry of the waveguide, a stratified film is bounded by a nonlinear cladding for $z \geq 0$ and a dielectric substrate for $z \leq -d$, the values of ε_1, ε_2 and ε_3 are 2.4, 2.4025, and 1 respectively and d=20 $\times 10^{-6}$ m

Field equations and boundary conditions:

The electric and magnetic field vectors for TE waves propagating along the x-axis with angular frequency ω and wave number k are as follows;

$$E = [0, E_y(\omega, z), 0]\, e^{i(kx - \omega t)}$$
$$H = [H_x(\omega, z), 0, H_z(\omega, z)]\, e^{i(kx - \omega t)} \tag{1}$$

In this paper TE waves will be only considered.
Maxwell's equations for fields propagating on the media are

$$\vec{\nabla} \times \vec{E} = -i\omega\mu_0 \vec{H}$$
$$\vec{\nabla} \times \vec{H} = i\omega\varepsilon_0 \varepsilon_{mi} \vec{E}$$
$$\frac{\partial E_y}{\partial z} = i\omega\mu_0 H_x$$
$$kE_y = -\omega\mu_0 H_z$$
$$\frac{\partial H_x}{\partial z} - ikH_z = i\omega\varepsilon_0\varepsilon_{mi} E_y \tag{2}$$

where ε_{mi} is the relative dielectric with i=1, 2, 3 for medium-1, medium-2 and medium-3, respectively.

Applying the fields as presented in Equation (1) into Equation (2) the field equation for each medium can be derived.

For medium-2:

$$\frac{\partial H_x}{\partial z} - ikH_z = i\omega\varepsilon_0[\varepsilon_2 + \Delta\cos\delta z]E_y \ ,$$
$$\frac{1}{\iota\omega\mu_0}\left[\frac{\partial^2 E_y}{\partial z^2}\right] + \frac{\iota k^2}{\omega\mu_0}E_y = \iota\omega\varepsilon_0\left[\varepsilon_2 + \Delta\cos\delta z\right]E_y \ ,$$
$$\frac{\partial^2 E_y}{\partial z^2} - k^2 E_y = -\left[k_0^2\varepsilon_2 + k_0^2\Delta\cos\delta z\right]E_y \ ,$$
$$\frac{\partial^2 E_y}{\partial z^2} - k^2 E_y + k_0^2\varepsilon_2 E_y + k_0^2\,\Delta\cos\delta z\ E_y = 0,$$

$$\frac{\partial^2 E_y}{\partial z^2} + \left[k_0^2 \varepsilon_2 - k^2\right] E_y + k_0^2 \, \Delta \cos \delta z \quad E_y = 0,$$

If we change the variable δz by $2z$, and $K^2 = k_0^2 \varepsilon_2 - k^2$

The field equation in medium-2 will take the following form:

$$\frac{d^2 E^{(2)}}{dz^2} + \left(a - 2q \cos 2Z\right) E^{(2)} = 0, \tag{3}$$

where

$$a = \frac{4K^2}{\delta^2} \quad , \quad q = - \frac{2\Delta k_0^2}{\delta^2}$$

This is well known as Mathieu differential equation with negative q [8-9].

For medium-1:
Following similar steps, we end with a field equation with a well-known solution of the form [7]:

$$E_y^{(1)} = \sqrt{\frac{2}{\alpha}} \; \frac{q_c}{\cosh\left(k_0 q_c \left(z + z_c\right)\right)}, \tag{4}$$

where $q_c = \frac{k}{k_0} = \sqrt{\beta^2 - \varepsilon_1}$ and β is the effective index.

For medium-3:
Following similar steps, we get the field equation with a well-known solution of the form :

$$E_y^{(3)} = B \, e^{K_3 (z - d)}, \tag{6}$$

where $K_3 = k_0\sqrt{\beta^2 - \varepsilon_3}$ and B is the value of the electric field at the lower boundary of the film.

Power Calculations:

The power flow in medium-1(cladding) is

$$p_1 = \frac{\beta k_0}{2\omega\mu_0}\int_0^{\infty} (E^{(1)})^2 \, dz \,, \tag{7}$$

$$p_1 = \frac{\beta q_c}{\omega \mu_0 \alpha}\left[1 - \tanh(k_0 q_c z_c)\right], \tag{8}$$

Where Z_c=1.2 $\times 10^{-6}$, $c=3\times10^{8}$, $\mu_0=4\pi\times10^{-4}$, Λ=1.5μm. Power flow in medium-1 as a function of β is shown in Figure (2)

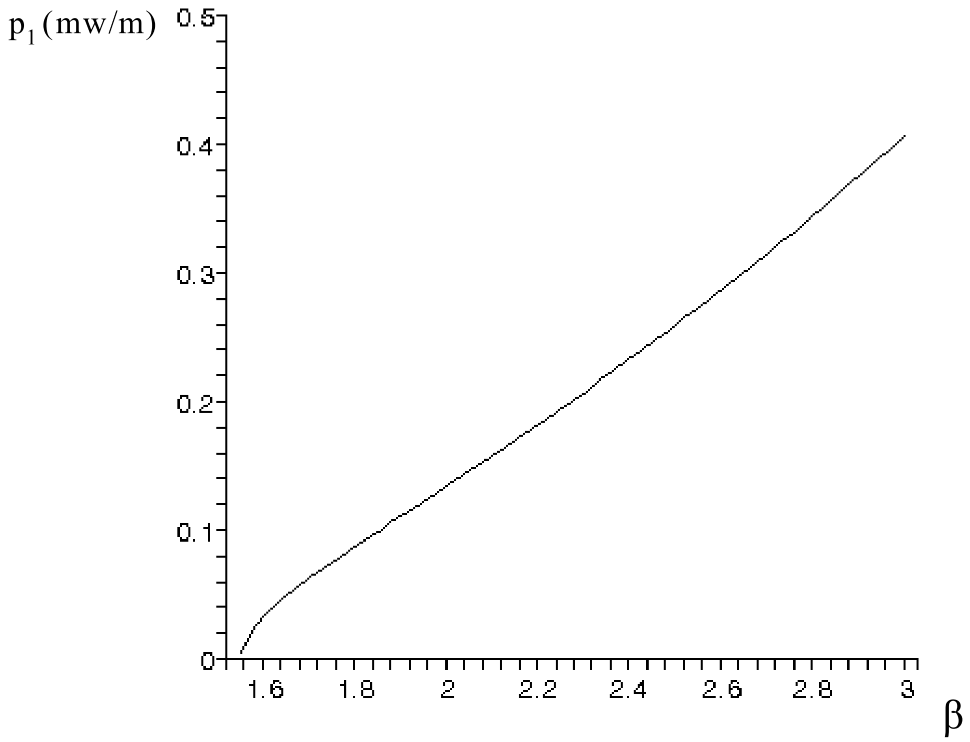

Figure 2. Cladding power versus β for ω=1.5 ×10^12 rad/s.

The power flow in medium-3 is:

$$p_3 = \frac{\beta k_0}{2\omega\mu_0} \int_{-\infty}^{d} (E^{(3)})^2 \, dz ,$$

$$p_3 = \frac{\beta k_0 B^2}{4\omega\mu_0 K_3} . \tag{9}$$

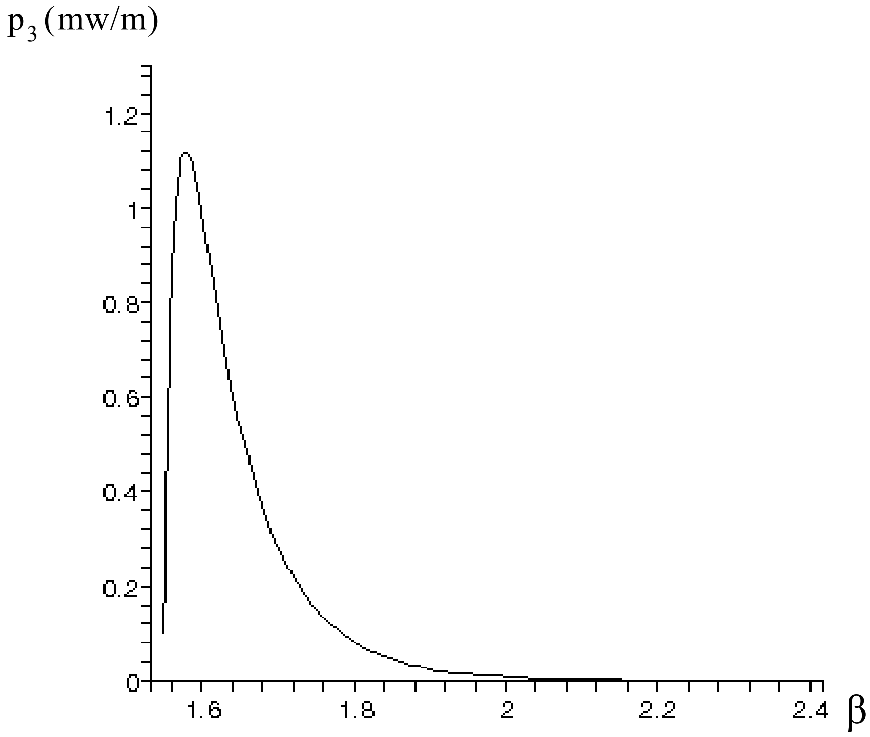

Figure (3). Power flow in medium-3 versus β for ω=1.5 ×10^{12} rad/s.

Power flow in medium-3 is calculated as function of β and plotted as shown in Figurer (3).

Power Flow in Medium-2

a) Using Mathieu function:

The exact solution for Mathieu equation using Mathieu function ce_r, se_r

as [8-9] :

$$E_y = C\ (ce_r(z,q) \ + se_r(z,q)), \tag{10}$$

where C is a constant to be determined from the boundary condition. The power flow in medium-2 is :

$$p_2 = \frac{k}{2\omega\mu_0} \int_{-d}^{0} (E_y)^2 \ \mathrm{dz}. \tag{11}$$

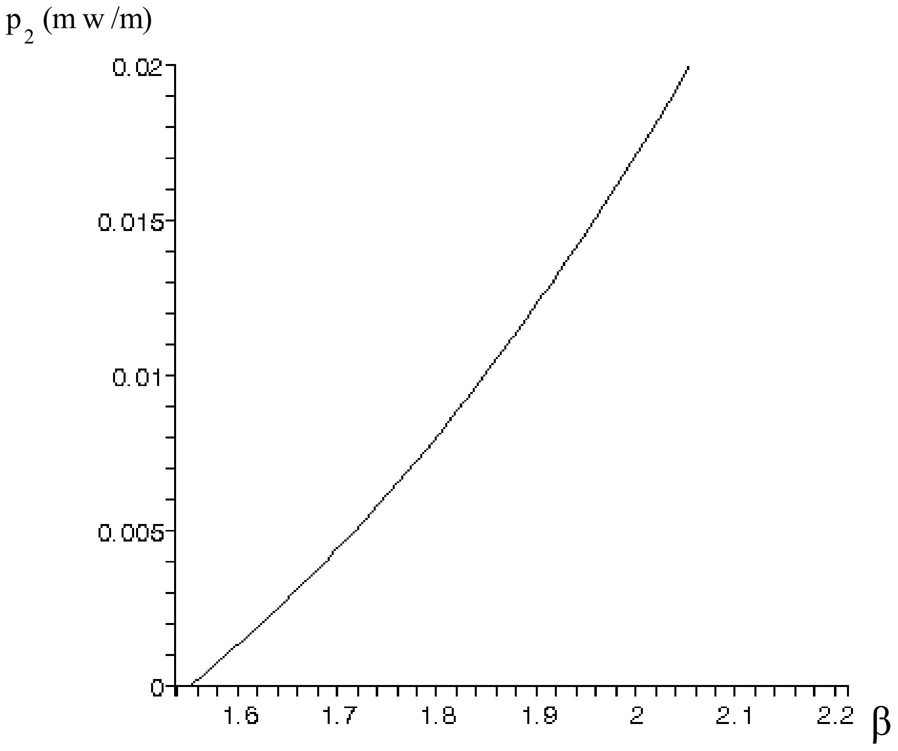

Figure (4). Power flow in medium-2 calculated using exact solution by Mathieu functions versus β for ω=1.5 ×10^{12} rad/s.

Power flow propagating in medium-2 which is calculated using as function of β is illustrated in Figure (4).

b)Using Whittaker's Method,:

In medium-2, the field equation with positive q is:

$$\frac{d^2 E_y^{(2)}}{dZ^2} + \left(a + 2q \cos 2Z\right) E_y^{(2)} = 0. \tag{12}$$

In this case we use the normal or floquet forms of the solution [16] and the electric field takes this form: $E_y^{(2)}(z) = e^{\gamma z}\,\phi(z)$,

where $\phi(z+2\pi) = \phi(z)$ according to Floquet theory.

Substituting the electric field into Equation (12), then expanding ø(z), a and γ in terms of q, we get:

$$ø(z,q) = ø_0(z) + q\, ø_1(z) + q^2 ø_2(z) + \ldots.$$

$$a = a_0 + q a_1 + q^2 a_2 + \ldots\ldots$$

$$\gamma = q\gamma_1 + q^2 \gamma_2 + \ldots\ldots \tag{13}$$

And keeping only O(q) and for n=1 , the general solution of Eq. (12) will be :

$$E_y = d_1\, e^{\frac{\delta q}{4}\sqrt{1-a_1^2}\, z} \left[\cos\frac{\delta z}{2} - \left(\frac{1+a_1}{1-a_1}\right)^{\frac{1}{2}} \sin\frac{\delta z}{2}\right]$$

$$+\, d_2\, e^{-\frac{\delta q}{4}\sqrt{1-a_1^2}\, z} \left[\cos\frac{\delta z}{2} + \left(\frac{1+a_1}{1-a_1}\right)^{\frac{1}{2}} \sin\frac{\delta z}{2}\right] \tag{14}$$

The constants d_1 and d_2 will be determined from the boundary conditions.

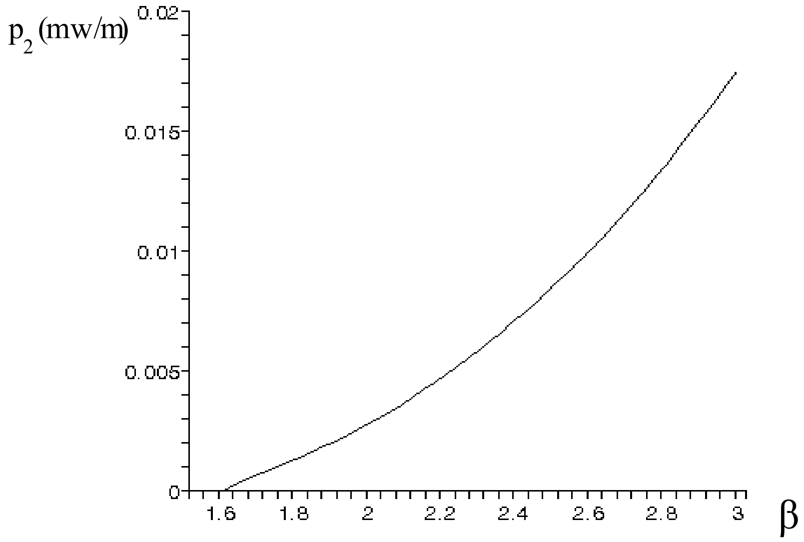

Figure (5). Power flow in medium-2 calculated using approximate methods versus β for ω=1.5 ×10^{12} rad/s.

Equation (11) is used to calculate the power flow in medium. Results are demonstrated in Figure (5).

c) Using the Multiple Scale Method:

The multiple scales method is used to solved Mathieu equation without the need to know the form of the solution (more advance methods) [16].
To apply the method of multiple scales to solve Mathieu equation Equation (3) we seek a uniform expansion in the form shown in Equation (11) :

$$\begin{aligned} E(z;q) &= E(Z_0, Z_1, Z_2, \ldots\ldots\ldots, Z_n, q) \\ &= E_0 + qE_1 + q^2 E_2 + \ldots\ldots\ldots \end{aligned} \tag{15}$$

where $Z_n=q^n z$

We obtain only a first-order expansion, thus we stop at o(q) and use only z_0 and z_1.

$$\frac{d}{dz} = D_0 + qD_1 + qD_2 + ...$$

$$\frac{d^2}{dz^2} = D_0^2 + 2qD_0D_1 + q^2(D_1 + 2D_0D_2) + ... \tag{16}$$

Where $D_n = \frac{\partial}{\partial Z_n}$. Substituting Equation (15) and Equation (16) into Equation (12) we obtain to the first approximation:

$$E_y = d_1 \, e^{(\frac{q}{4}\delta\sqrt{1\text{-}4\omega_1^2}\,)Z} \left(\cos\frac{\delta}{2} z - \sqrt{\frac{1+2\omega_1}{1-2\omega_1}} \sin\frac{\delta}{2} z \right)$$

$$+ d_2 \, e^{(-\frac{q}{4}\delta\sqrt{1\text{-}4\omega_1^2}\,)Z} \left(\cos\frac{\delta}{2} z + \sqrt{\frac{1+2\omega_1}{1-2\omega_1}} \sin\frac{\delta}{2} z \right) \tag{17}$$

which agreement with Equation (14) when $2\omega_1 = a_1$, d_1 and d_2 are constants can be calculated from the boundary condition at z=0 and z=-d.

at z=0, the boundary conditions is: $E_y^{(1)} = E_y^{(2)}$, $H_x^{(1)} = H_x^{(2)}$.

And z= - d, the boundary condition is: $E_y^{(2)} = E_y^{(3)}$, $H_x^{(2)} = H_x^{(3)}$.

The dispersion equation is derived from the boundary condition

$$d_1\left[K_3 - h\right] e^{2hd} \left[\cos\frac{\delta d}{2} - A\sin\frac{\delta d}{2}\right] + d_2\left[K_3 + h\right]\left[\cos\frac{\delta d}{2} + A\sin\frac{\delta d}{2}\right]$$

$$= d_2\frac{\delta}{2}(-\sin\frac{\delta d}{2} + A\cos\frac{\delta d}{2}) - d_1\frac{\delta}{2}e^{2hd}(\sin\frac{\delta d}{2} + A\cos\frac{\delta d}{2}), \tag{18}$$

where $h = \frac{\delta q}{4}\sqrt{1-a_1^2}$ and $A = \left(\frac{1+a_1}{1-a_1}\right)^{\frac{1}{2}}$ · Equation (18) relates d_1 and d_2 and solved numerically.

The power flow has been calculated using Mathieu's function, and the result comes close to the result that has been calculated using Whittaker's method and Multiple-scale method, as shown in Figures (4) and (5).

Total Power Calculation:

The total power flow has been calculated using Maple 9 using the three techniques described for calculating the power in medium-2. The total power flow is calculated as $P_t = P_1 + P_2 + P_3$. Results show that there is a great agreement between the exact solution (Mathieu's function) and approximate methods (perturbation methods). Plots of the total power flow versus relative refractive index β using Mathieu's function as shown in Figures (6), and using the approximate solution as shown in Figure (7). Figures (8) compare the results of total power flow as function of β as calculated using different methods.

The total power flow is plotted as a function of frequencies at different values of effective refractive indices (e.g. β_1=1.6, β_2=1.7, β_3=1.8, β_4=2, β_5=2.3, β_6=2.5) for the exact calculation as in Figure (9) and approximate solution as in Figure (10). In Figure (11), same calculation is repeated for higher values of frequencies.

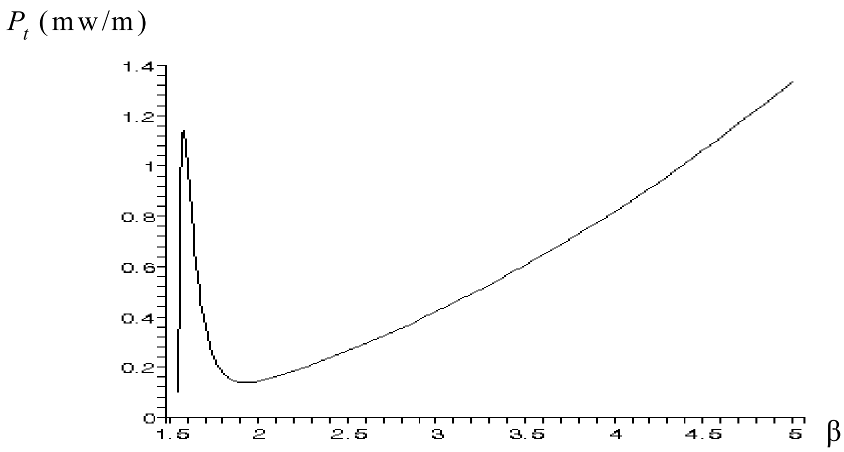

Figure (6). Total Power flow calculated using Mathieu function versus β for ω=1.5 ×10^{12} rad/s.

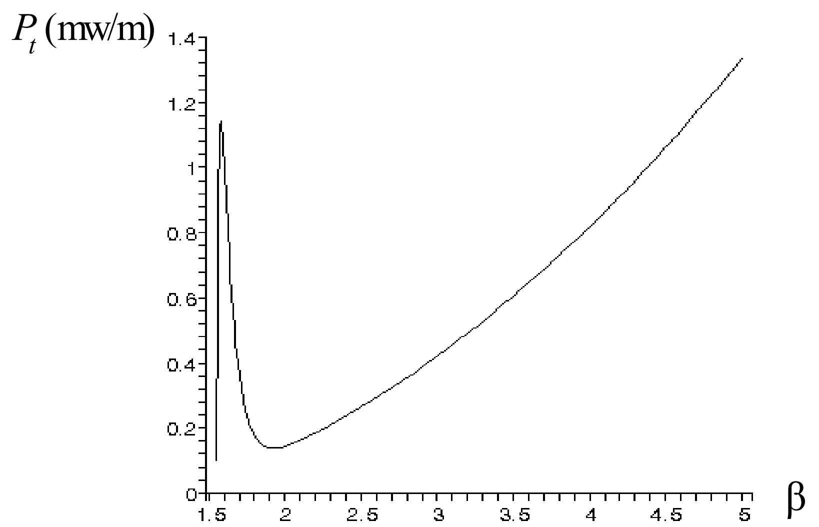

Figure (7). Total power flow calculated using approximate methods versus β for ω=1.5 ×10^{12} rad/s.

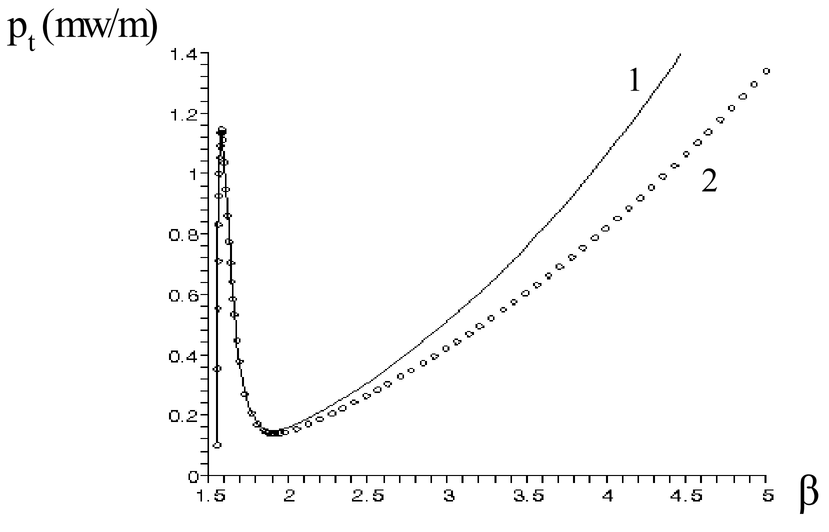

Figure (8): Total Power flow calculated using (1) Mathieu function (2) approximation method as function of β at ω=1.5 ×0^{12} rad/s.

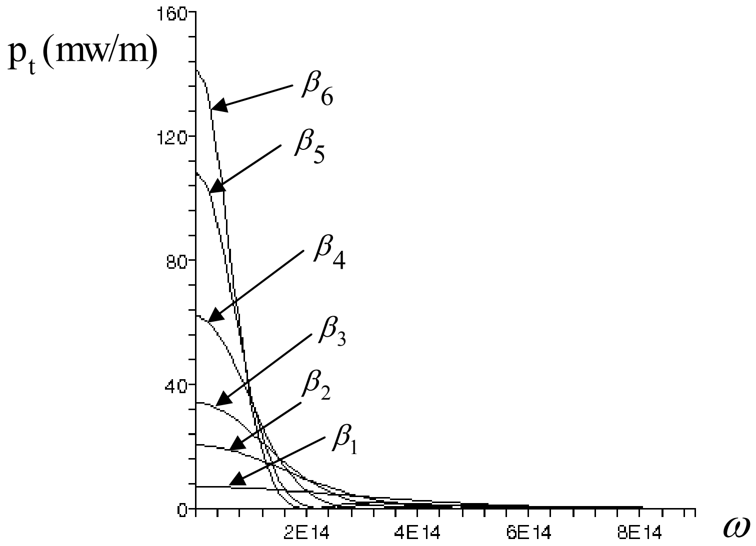

Figure (9): Total power versus frequency for different values of β calculated using Mathieu function where β_1=1.6, β_2=1.7, β_3=1.8, β_4=2, β_5=2.3, β_6=2.5.

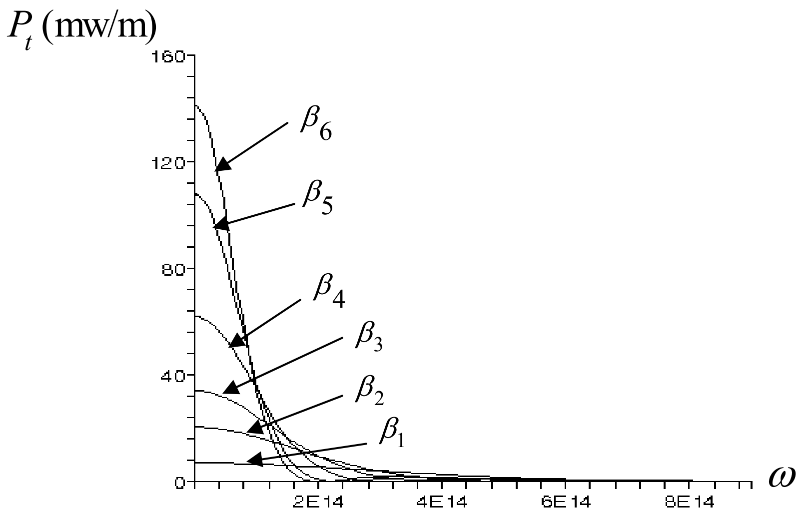

Figure (10): Total power flow versus frequency for different values of β calculated using approximate method where β_1=1.6, β_2=1.7, β_3=1.8, β_4=2, β_5=2.3, β_6=2.5.

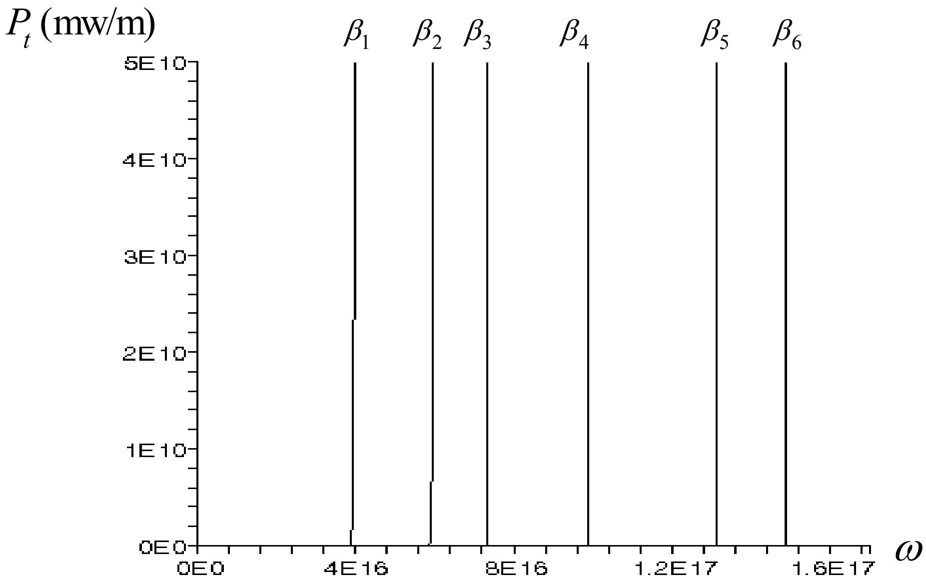

Figure (11). Total power flow versus frequency for different values of β where β_1=1.6, β_2=1.7, β_3=1.8, β_4=2, β_5=2.3, β_6=2.5.

RESULTS AND CONCLUSION:

Power flow in medium-1 as a function of β is shown in Figure (2). Figure (2) indicates that as power flow increases β increases. Figurer (3) shows the power flow in medium-3 as function of β. The figure indicates that as β increases power flow in medium-3 increases to a maximum value then decrease again. Power flow propagating in medium-2 calculated using Mathieu functions as function of β is plotted in Figure (4). Figure (4) demonstrates that β increase with increasing power flow. The power flow in medium-2 has been calculated using approximate methods, Whittaker's method and Multiple-scale method, and plotted as function of β as shown in Figures (4) and (5). The results of the power flow in medium-2 calculated using the exact comes close to the result of the one calculated using approximate solution which show that as the power flow increases the effective index β increases. As a result, we recommend using the approximation method to save time and avoid tedious calculations.

Total power flow calculated using Mathieu functions and using the approximate solution as function β of is shown in Figure (6) and Figure (7) respectively. Figures (8) compare the results of total power flow as function of β as calculated using different methods. Results show that there is a great agreement between the exact solution and the approximate solution.

The total power flow is plotted as a function of frequencies at different values of effective refractive indices (e.g. β_1=1.6, β_2=1.7, β_3=1.8, β_4=2, β_5=2.3, β_6=2.5) for the exact calculation as in Figure (9) and approximate solution as in Figure (10). In Figure (11), same calculation is repeated for higher values of frequencies. Results show that there is a stop band at the optical frequency at different values of β. Thus, the proposed configuration is recommended for designing band reject filter.

REFERENCES:

1. Rayleih L. and Mag. P. (1998): 24, 145–159.

2. Yariv A. and Yeh P. (1984): Optical Waves in Crystals: Propagation and Control of Laser Radiation, Wiley, New York.

3. Ariyasu J., Seaton C., Stegeman G. , Maradudin A., and Wallis R. (1985): J .App. Phys, vol. 58, 2460.

4. Vingogradov A. and Koyhevnikov I. (1984): JETP Lett. 40, 1221.

5. Popov V.(1987): Sov. Phys. Crystallogr. 32, 578 .

6. Belyakov V. and Orlov V. (1991): Mol. Cryst. Liq. Cryst. Lett. 8, 1 .
7. Stegeman G., Seaton C., Ariyasu J., Wallis R., and Maradudin A. (1985) : J. Appl. Pyhs., vol. 58(7).
8. Ruby L. (1996): Am. J. phys.64,39-44.
9. McLachlan N. (1995): Theory and Application of Mathieu Functions, Oxford.
10. Shabat M. , Barakat N. and Jäger D. (2002): Electromagnetic Journal, vol.22, no.8, 667-674.
11. Udoev Yu. (1988): Sov. Phys . Tech. Phys, vol.33(3), 368-370.
12. Tamir T. , Wang H. , and Oliner A. (1964): IEEE Trans. Microwave Theory Tech. 12 (3), 323-335 .
13. El-Khozondar H., El-Saifi R., and Shabat M. (2004): Laser Physics, vol.14 (12), 1539- 1543.
14. Kuchment P. (2004) : Waves in Periodic Media and Random Media, Eds., Texas University: Texas.
15. Mei C. (1995): Mathematical Analysis in Engineering, Cambridge University Press: New York .
16. Nayfeh A. (1981): Introduction to Perturbation Techniques, Wiley, New York.